

Supporting information

Novel luminescent β -ketoimine derivative of 2,1,3-benzothiadiazole: synthesis, complexation with Zn(II) and photophysical properties in comparison with related compounds

by

Taisiya S. Sukhikh, Denis A. Bashirov, Darya S. Ogienko, Natalia V. Kuratieva, Petr S. Sherin, Mariana I. Rakhmanova, Elena A. Chulanova, Nina P. Gritsan, Sergey N. Konchenko* and

Andrey V. Zibarev

Figure S1. UV-Vis spectra of L2H and L2⁻ . MOs for L2⁻	S2
Figure S2. The NMR spectra of L2H and ZnL2	S3
Figure S3. Calculation of thermodynamics of ZnCl ₂ complexation with L1 , L2H and L2⁻	S3
Figure S4. UV-Vis, fluorescence and excitation spectra of L1 and L2H	S4
Figure S5. UV-Vis spectrum of ZnL2 with a drop of water. Fluorescence decay of ZnL2	S5
Figure S6. IR spectra, powder XRD data and mass loss curves for L1 and ZnL1	S6
Table S1. Calculated wavelengths, oscillator strengths and major configurations for ZnL1 ..	S7
Figure S7. MOs involved in the lowest energy transitions of L1 and ZnL1	S7
Table S2. Calculated wavelengths, oscillator strengths and major configurations for ZnL2	S8
Figure S8. MOs of L2H , L2⁻ and ZnL2	S8
Figure S9. Fluorescence decay kinetics, TRES and DAS data for L1	S9
Figure S10. Fluorescence and excitation spectra of ZnL1 at different excitation and emission wavelengths. UV-Vis spectrum of ZnL1	S10
Figure S11. Fluorescence decay, TRES and DAS data for L2H and ZnL2	S11
Table S3. Crystallographic data for L2H - α , L2H - β and ZnL2	S12
Figure S12. Photographs of the samples of L1 , ZnL1 , L2H and ZnL2	S13

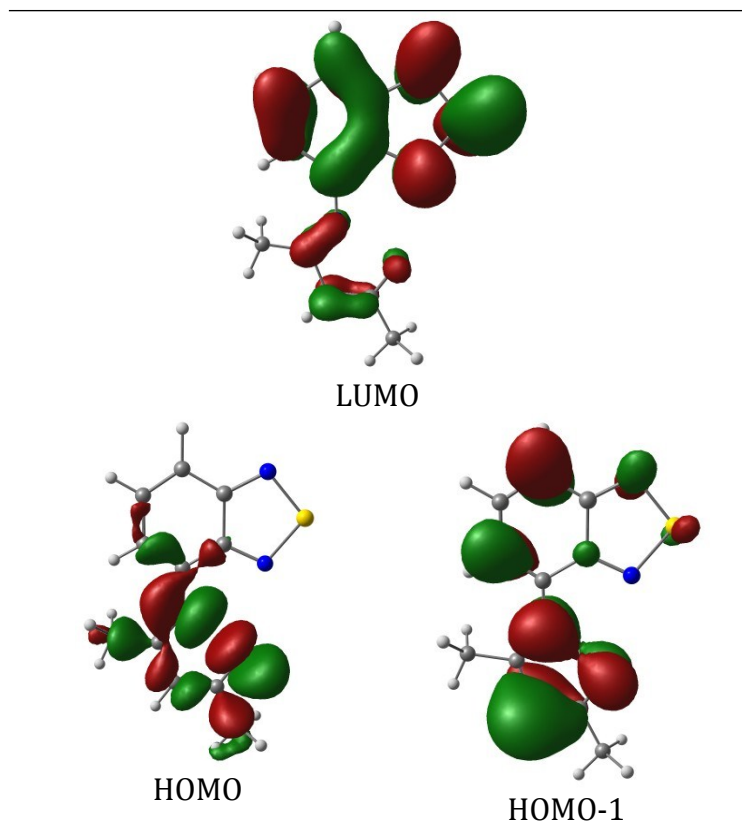
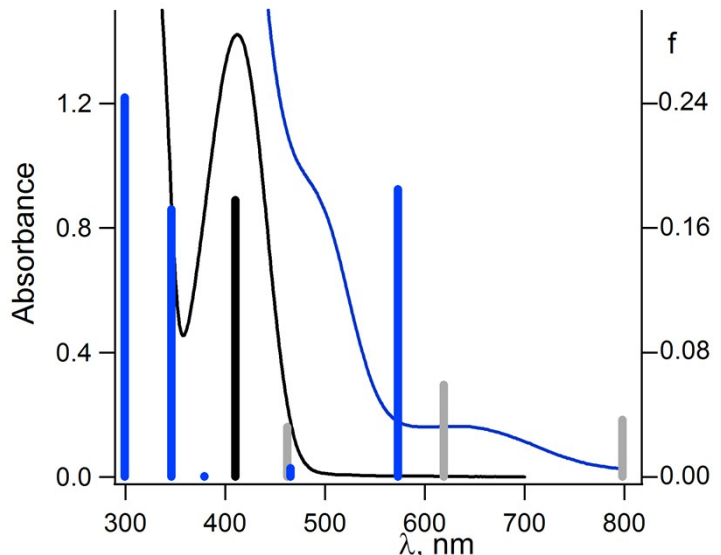


Figure S1. (Top) UV-Vis spectra of **L2H** (1.2×10^{-4} M, black curve) and its deprotonated form L2^- (blue curve) in CH_2Cl_2 in the presence of KO^tBu and 18-crown-6 ether (both $4.4 \cdot 10^{-2}$ M). Positions and oscillator strengths calculated at the TD-M06-HF/TZVP level of theory are depicted as solid bars for **L2H** (black) and for L2^- (blue bars – for geometry of L2^- optimized at B97-D3/TZVP level, gray bars – for geometry of L2^- from XRD of **ZnL2**. (Bottom) Molecular orbitals (MOs) involved in the lowest energy transitions for L2^- .

Calculation of the UV-Vis spectrum for optimized geometry of L2^- . The long-wavelength transition at 573 nm in the UV-Vis spectrum is due to the electron promotion from HOMO to LUMO. The next transition is mainly due to the electron promotion from HOMO-1 to LUMO, it is predicted at 465 nm. Both the HOMO and HOMO-1 are localized mainly on substituent while LUMO – almost exclusively on the BTD (Fig. S1, bottom).

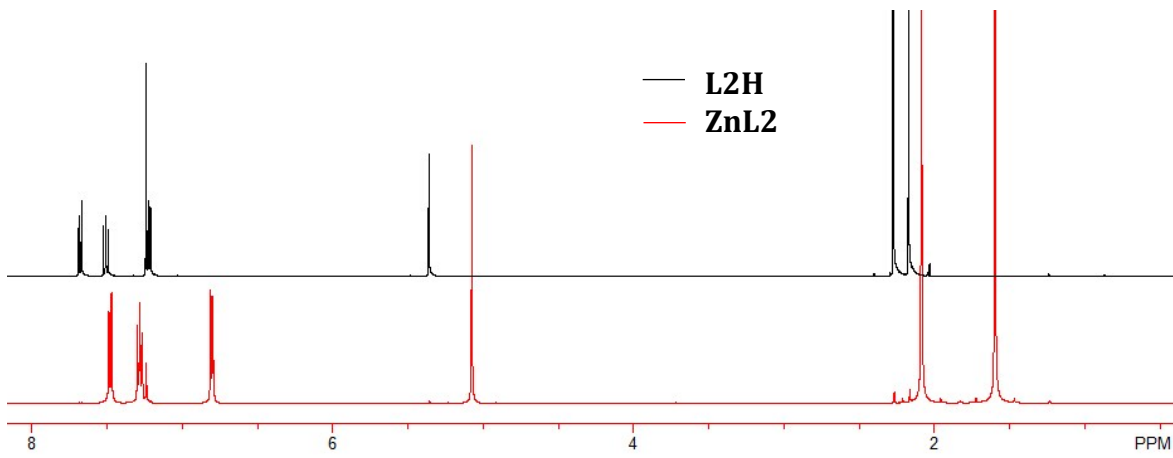


Figure S2. The NMR spectra of **L2H** and **ZnL2** in CDCl_3

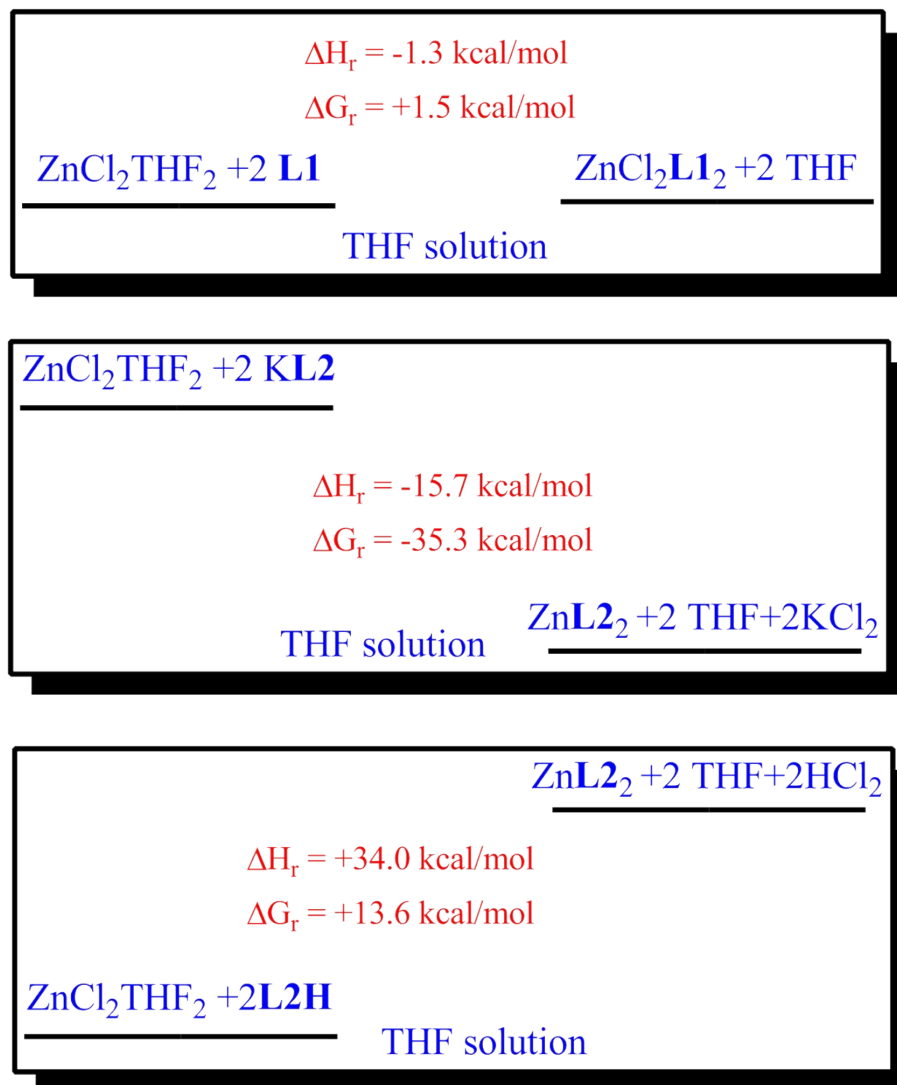


Figure S3. Thermodynamics of ZnCl_2 complexation with substituted BTD **L1**, **L2H** and **L2**—calculated at the B97D3/def2-TZVP level with account of solvent using COSMO model.

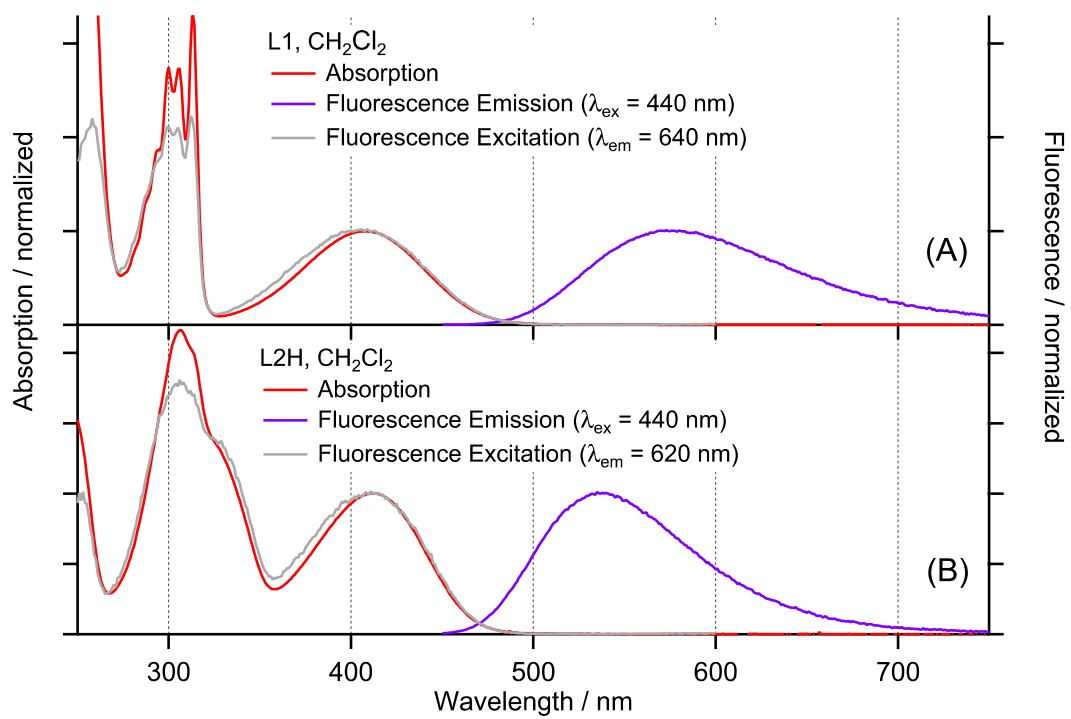


Figure S4. UV-Vis, fluorescence and excitation spectra of **L1**(A) and **L2H**(B) in CH_2Cl_2 at ambient temperature.

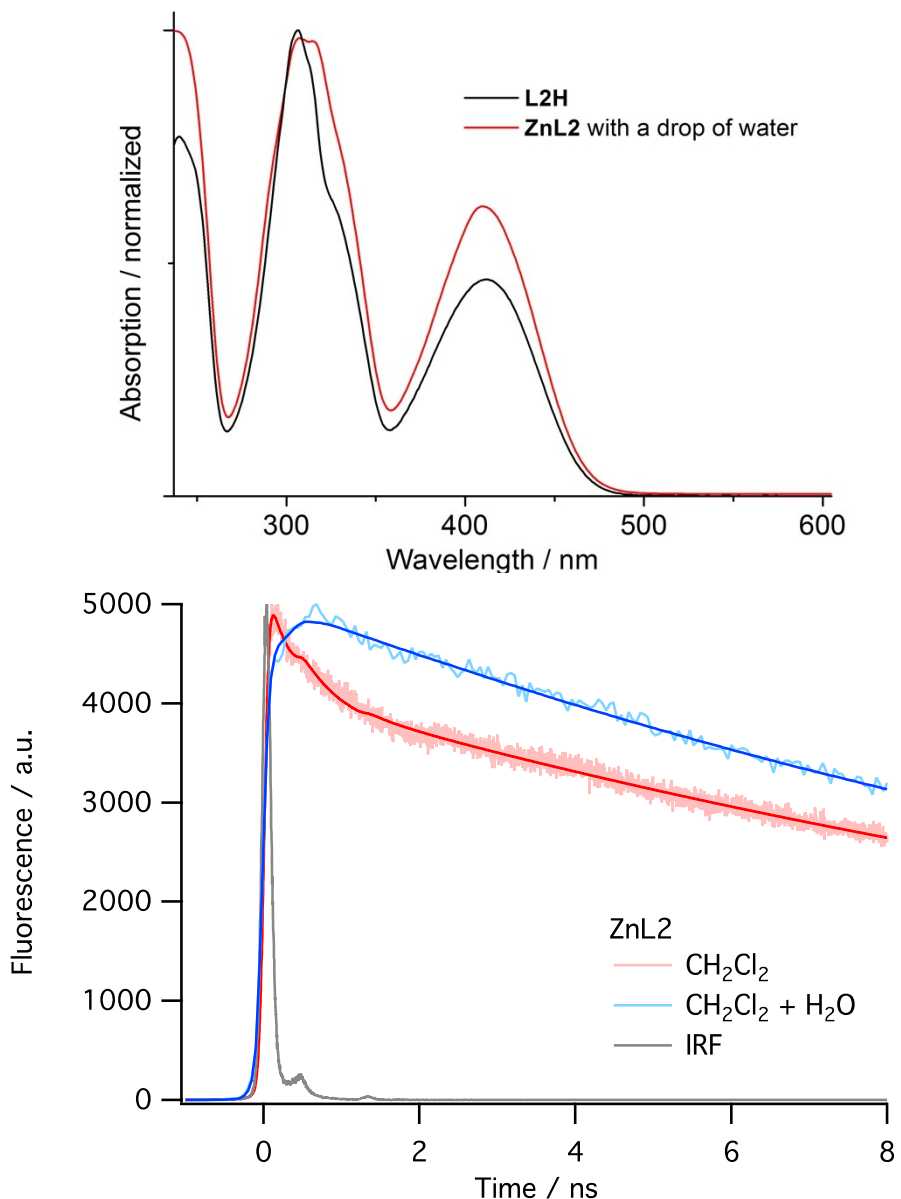


Figure S5. UV-Vis spectrum of **ZnL2** with a drop of water in comparison with **L2H** (A). Fluorescence decay kinetics of **ZnL2** in CH₂Cl₂ in the absence and presence of a drop of water (B).

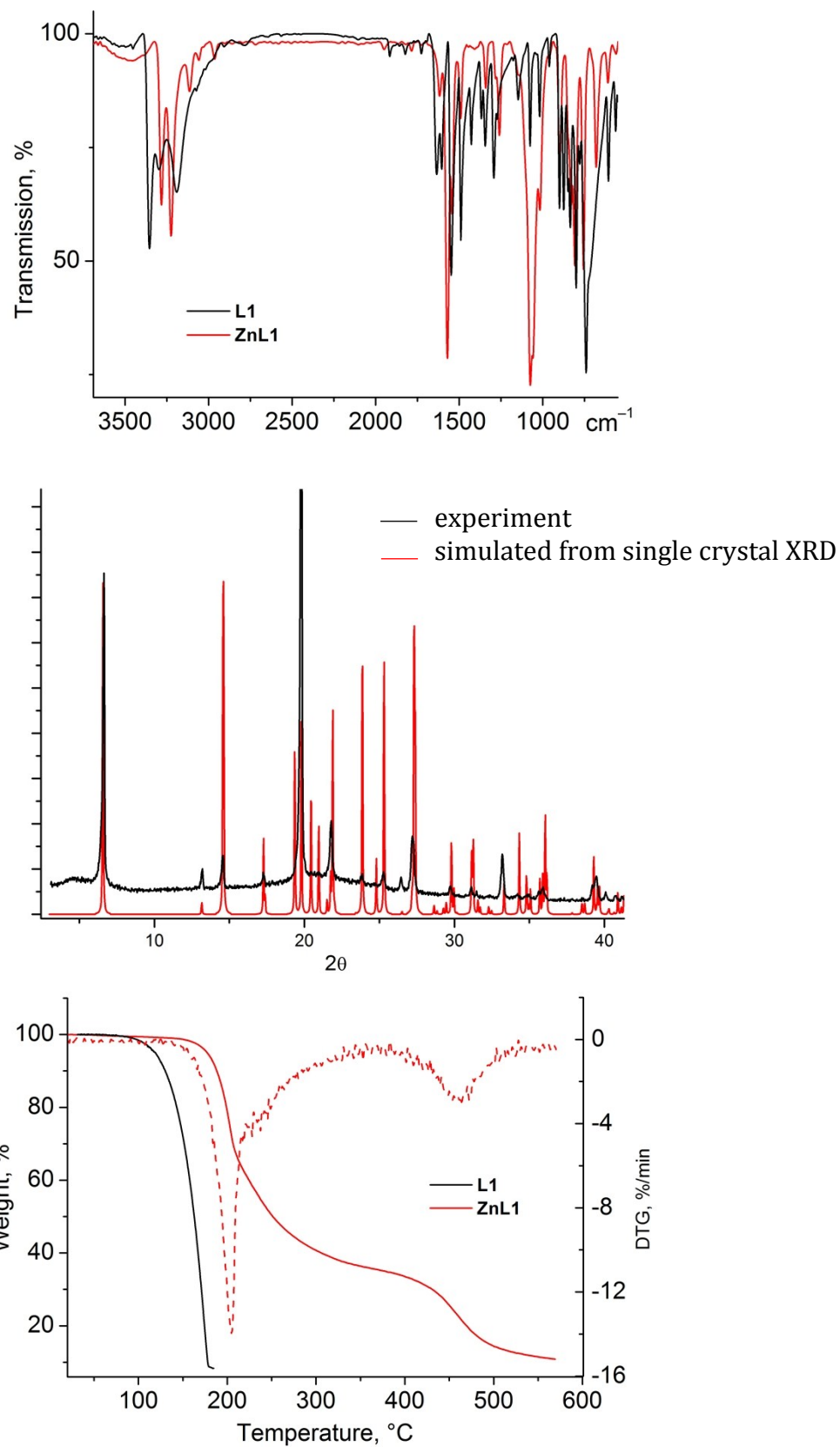


Figure S6. (Top) IR spectra of **L1** and **ZnL1**. (Middle) Experimental and simulated powder XRD data of **ZnL1**. (Bottom) Mass loss curves for **L1** and **ZnL1** (solid lines) and differential thermal analysis curve for **ZnL1** (dashed line).

Table S1. Wavelengths (λ_{\max}) of lowest energy electronic transitions, their oscillator strengths (f) and major configurations involved in these transitions for complex **ZnL1**.

λ_{\max} , nm	f	Major configurations
359	0.016	0.19(HOMO-1→LUMO+1)+0.68(HOMO→LUMO)
354	0.001	0.30(HOMO-1→LUMO)+0.64(HOMO→LUMO+1)
342	0.010	0.56(HOMO-1→LUMO)-0.28(HOMO→LUMO+1)+ 0.23(HOMO-2→LUMO+1)+0.18(HOMO-3→LUMO)
341	0.076	0.51(HOMO-1→LUMO+1)+0.44(HOMO-2→LUMO)+ 0.14(HOMO→LUMO)

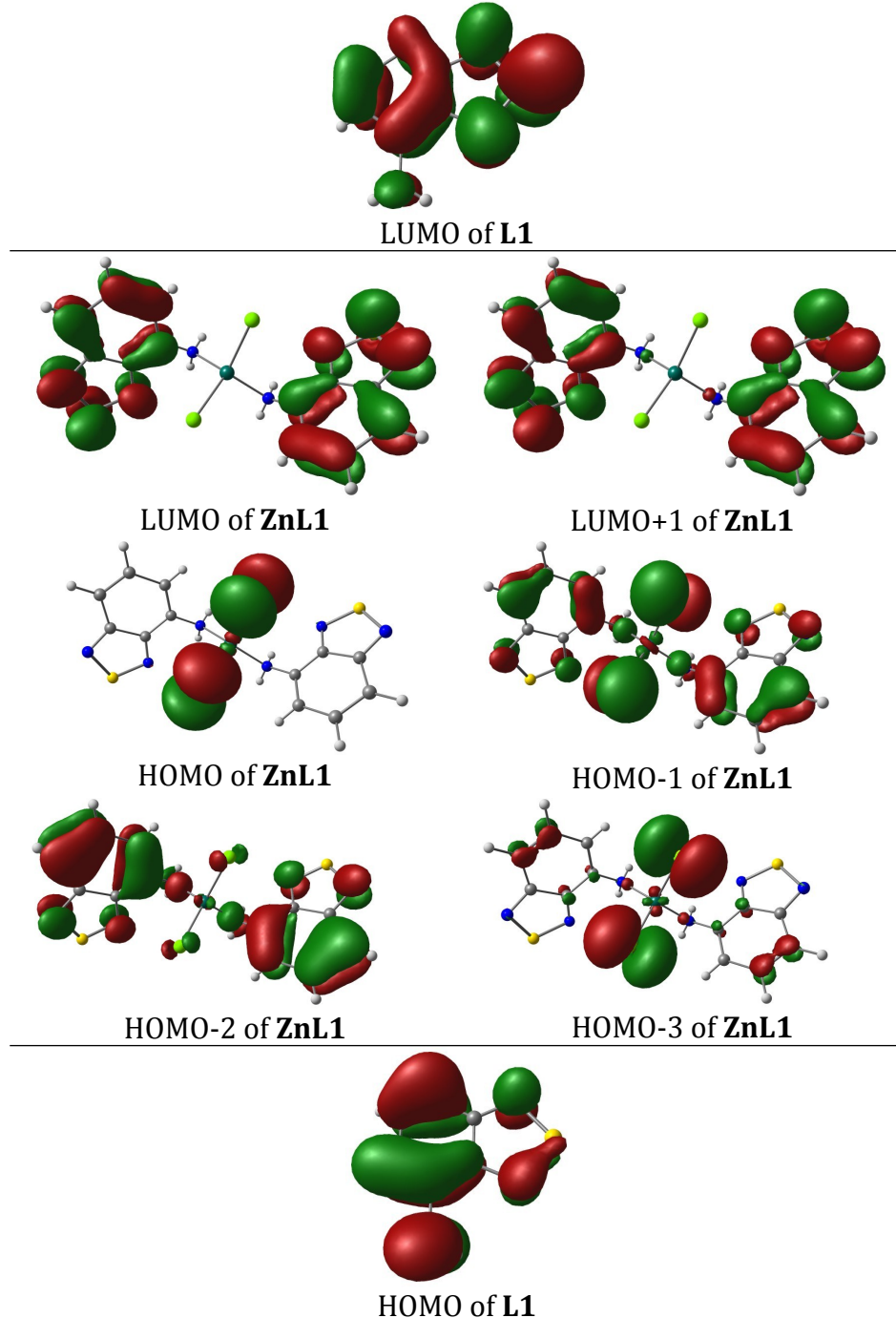
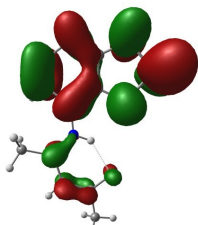


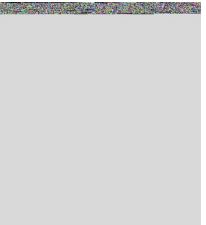
Figure S7. MOs involved in the lowest energy transitions of **L1** and **ZnL1**.

Table S2. Wavelengths (λ_{\max}) of lowest energy electronic transitions, their oscillator strengths (f) and major configurations involved in these transitions for complex **ZnL2**.

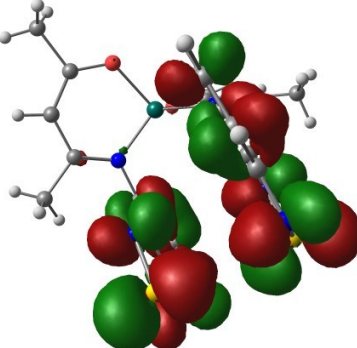
λ_{\max} , nm	f	Major configurations
430	0.059	0.20(HOMO-1 → LUMO+1)+0.68(HOMO → LUMO)
426	0.050	0.61(HOMO-1 → LUMO)+0.36(HOMO → LUMO+1)
408	0.011	-0.36(HOMO-1 → LUMO)+0.61(HOMO → LUMO+1)
403	0.020	0.66(HOMO-1 → LUMO+1)-0.20(HOMO → LUMO)



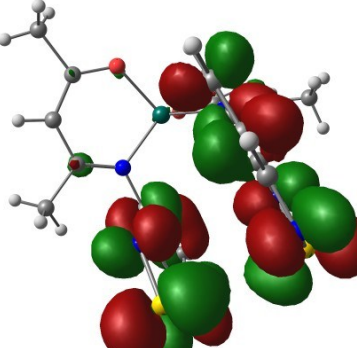
LUMO of **L2H**



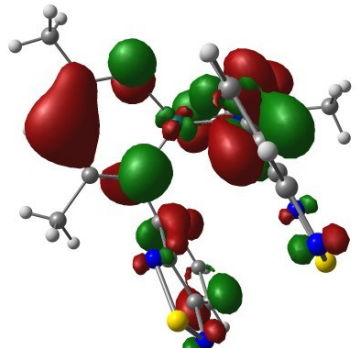
LUMO of **L2⁻**



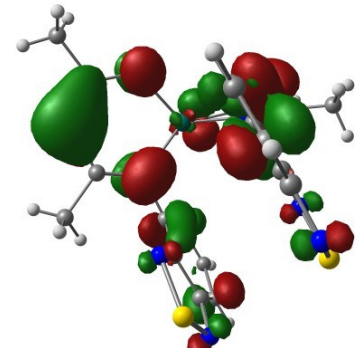
LUMO of **ZnL2**



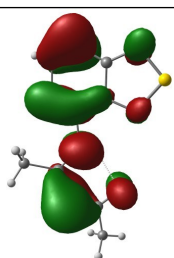
LUMO+1 of **ZnL2**



HOMO of **ZnL2**



HOMO-1 of **ZnL2**



HOMO of **L2H**



HOMO-1 of **L2⁻**

Figure S8. Molecular orbitals (MOs) involved in the lowest energy transitions of **L2H**, **L2⁻** and **ZnL2**.

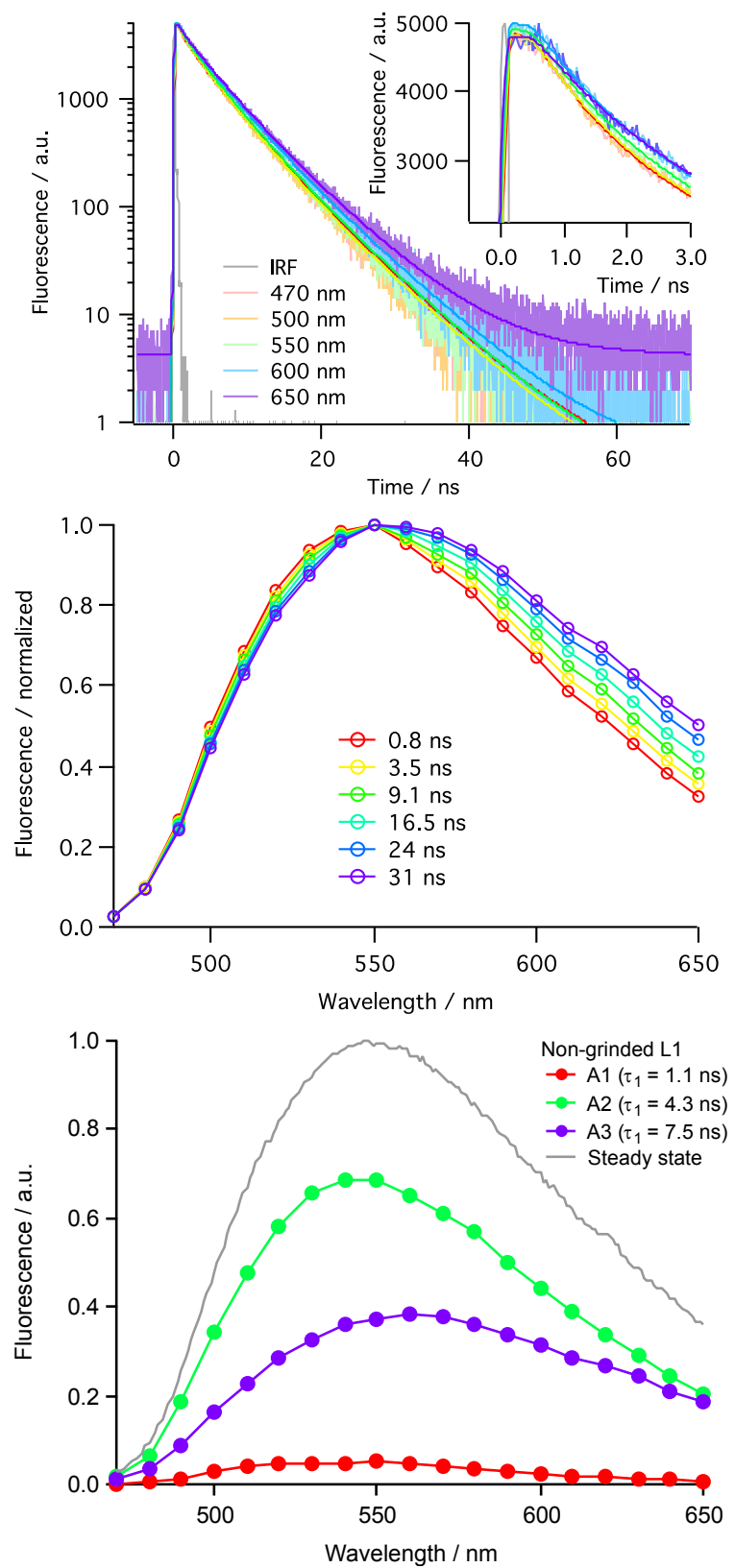


Figure S9. Fluorescence decay kinetics recorded over the emission band after the excitation of the polycrystalline samples of **L1** at 375 nm (top), intensity normalized Time Resolved Emission Spectra (TRES, middle) and Decay Associated Spectra (DAS, bottom) obtained from the analysis of decay kinetics.

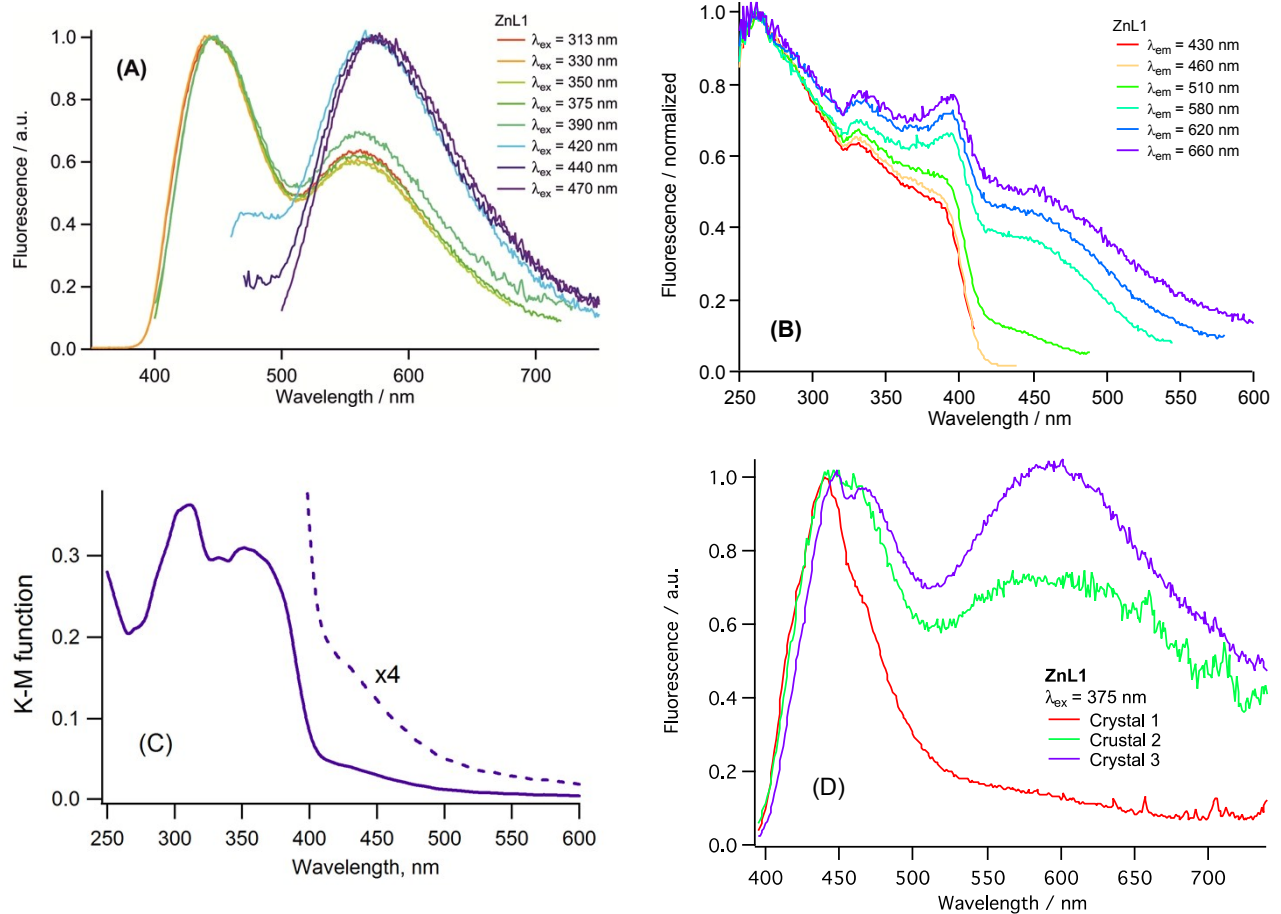


Figure S10. Fluorescence (A) and excitation (B) spectra recorded with polycrystalline **ZnL1** at different excitation (A) and emission (B) wavelengths. (C) UV-Vis spectrum of polycrystalline sample of **ZnL1** in the form of Kubelka-Munk function. (D) Fluorescence spectra of different crystals of **ZnL1**.

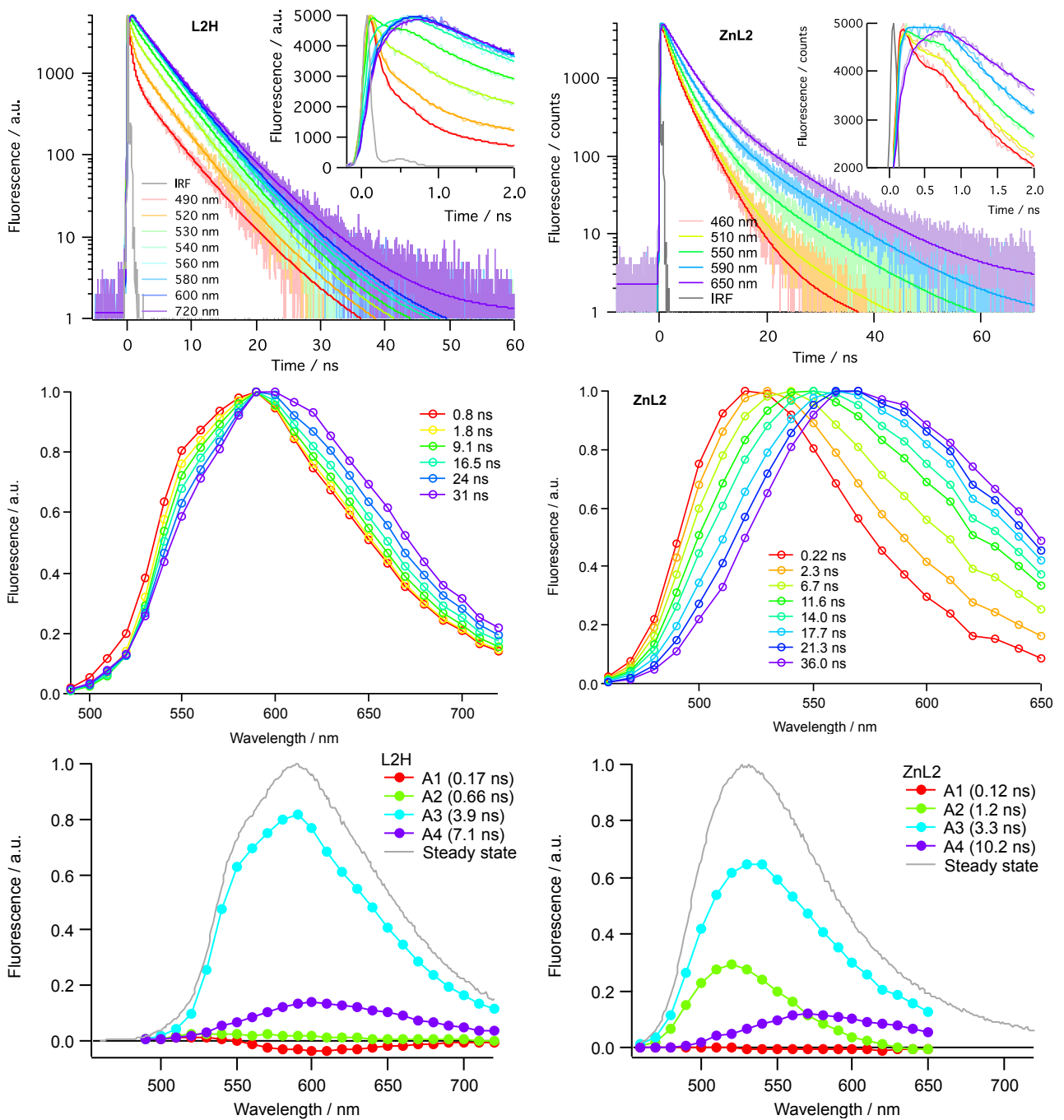


Figure S11. Fluorescence decay kinetics recorded over the emission band after the excitation at 375 nm (top), intensity normalized TRES (middle) and DAS (bottom) for the polycrystalline samples of **L2H** (left) and **ZnL2** (right).

Table S3. Crystallographic data of compounds α -L2H, β -L2H and ZnL2.

Compound	α-L2H	β-L2H	ZnL2
Empirical formula	C ₁₁ H ₁₁ N ₃ OS	C ₁₁ H ₁₁ N ₃ OS	C ₂₂ H ₂₀ N ₆ O ₂ S ₂ Zn
Formula weight	233.29	233.29	529.93
Crystal system	Orthorhombic	Monoclinic	Monoclinic
Space group	Pbca	P2 ₁ /c	C2/c
Unit cell dimensions <i>a</i> [Å]	7.1114(2)	14.9956(4)	7.3121(7)
<i>b</i> [Å]	14.9091(4)	10.8026(3)	22.517(2)
<i>c</i> [Å]	20.5365(6)	13.3402(3)	13.9416(12)
α [°]	90	90	90
β [°]	90	91.279(1)	93.916(3)
γ [°]	90	90	90
Volume [Å ³]	2177.37(11)	2160.46(10)	2290.1(4)
<i>Z</i>	8	8	4
Density (calcd.) [g cm ⁻³]	1.423	1.434	1.537
<i>F</i> (000)	976	976	1088
Abs. coefficient [mm ⁻¹]	0.278	0.280	1.288
Crystal size [mm ³]	0.42x0.25x0.04	0.30x0.17x0.11	0.27x0.22x0.18
2θ _{max} [°]	55.02	61.02	55.54
Index range	-9<=h<=8 -18<=k<=19 -26<=l<=26	-19<=h<=21 -15<=k<=15 -17<=l<=18	-9<=h<=9 -29<=k<=29 -17<=l<=18
Reflections collected	18512	21035	11631
Independent reflections	2505 [R(int) = 0.0436]	6080 [R(int) = 0.0256]	2645 [R(int) = 0.0396]
Completeness to 2θ = 50.5°[%]	99.9	100.0	99.0
Reflections, <i>I</i> ≥ 2σ(<i>I</i>)	2505	6080	2645
Parameters	147	293	152
Final R indices [<i>I</i> > 2σ(<i>I</i>)]	R1 = 0.0400, wR2 = 0.1048	R1 = 0.0372, wR2 = 0.0961	R1 = 0.0400, wR2 = 0.0962
R indices (all data)	R1 = 0.0567, wR2 = 0.1120	R1 = 0.0516, wR2 = 0.1014	R1 = 0.0511, wR2 = 0.1002
GoF	1.054	1.054	1.063
Residual electron density (min / max, e/Å ³)	-0.327 / 0.237	-0.257 / 0.454	-0.391 / 1.479

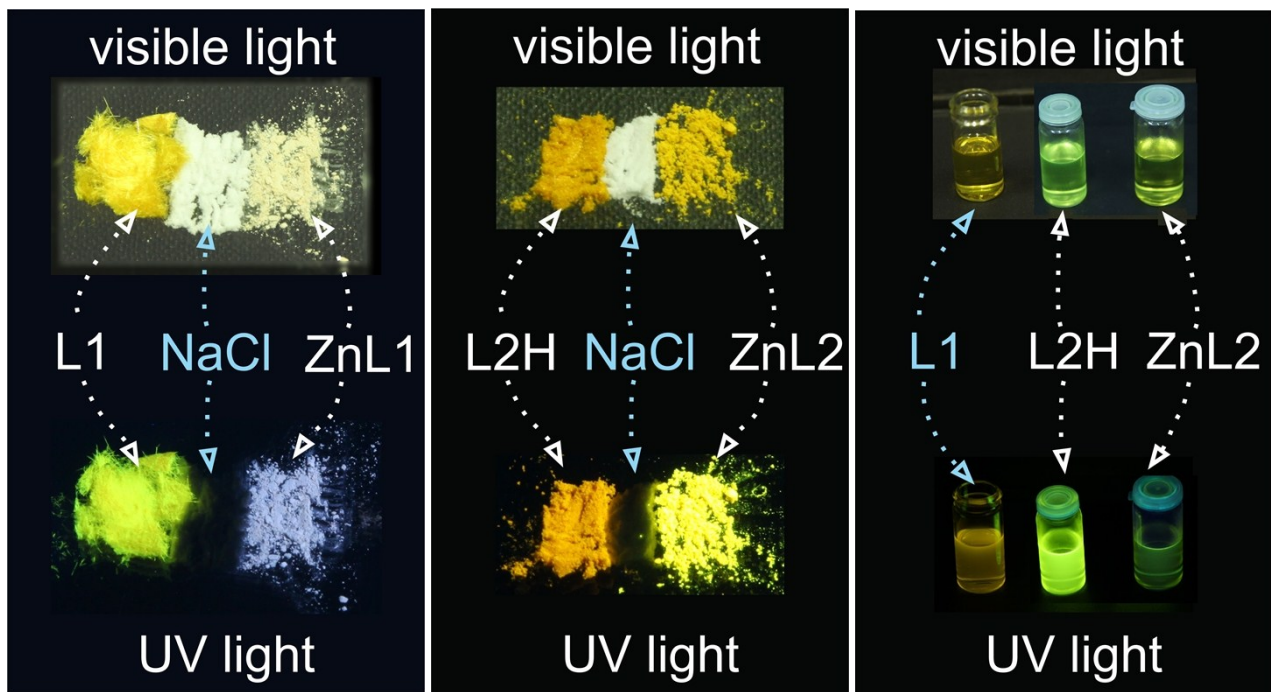


Figure S12. Photographs of solid **L1**, **ZnL1** (right), **L2H** and **ZnL2** (middle), NaCl is given as the substance of white color. Photographs of the solutions of **L1**, **L2H** and **ZnL2** in CH₂Cl₂. All samples are irradiated by visible (top) and ultraviolet (bottom) light.